View Article Online / Journal Homepage / Table of Contents for this issue
Dynamic Article Links

Dalton Transactions

Cite this: *Dalton Trans.*, 2011, **40**, 5528

www.rsc.org/dalton

PAPER

Published on 19 April 2011. Downloaded by Heinrich Heine University of Duesseldorf on 24/05/2013 13:04:26.

Coordination polymers of macrocyclic oxamide with 1,3,5-benzenetricarboxylate: syntheses, crystal structures and magnetic properties†

Ya-Qiu Sun,*[a] Dong-Zhao Gao,[a] Yan-Yan Xu,[a] Guo-Ying Zhang,[a] Lan-Lan Fan,[a] Cheng-Peng Li,[a] Tong-Liang Hu,[b] Dai-Zheng Liao[b] and Chen-Xi Zhang[c]

Received 15th November 2010, Accepted 17th March 2011
DOI: 10.1039/c0dt01584a

Solvothermal reactions of mixed ligands H_3BTC and macrocyclic oxamide complexes (ML, M = Cu, Ni) with $M(ClO_4)_2{\cdot}6H_2O$ (M = Co, Zn, Ni and Cd) afford six new complexes, including $[M'_4(BTC)_2(ML)_2(OH)_2(H_2O)_2]{\cdot}2H_2O$ (M′ = Co, M = Ni, for (**1**); M′ = Zn, M = Ni, for (**2**); M′ = Zn, M = Cu, for (**3**)), $[Ni_3(BTC)_2(NiL)_2(H_2O)_6]{\cdot}2CH_3OH{\cdot}2H_2O$ (**4**), $[Cd_4(BTC)_2(HBTC)(NiL)_4(H_2O)]{\cdot}3H_2O$ (**5**) and $[Cd(HBTC)(CuL)]{\cdot}H_2O$ (**6**) (ML, H_2L = 2, 3-dioxo-5, 6, 14, 15-dibenzo-1,4,8,12-tetraazacyclo-pentadeca-7,13-dien; H_3BTC = 1,3,5-benzenetricarboxylic acid). Complexes **1–3** consist of a 2D layer framework formed by the linkage of M(II)(M = Ni, Cu) and M'_4 (M′ = Co, Zn) cluster *via* the oxamide and BTC^{3-} bridges and display a (3,6)-connected network with a $(4^3)_2(4^6.6^6.8^3)$ topology. The structure of **4** consists of pentanuclear $[Ni^{II}_5]$ units and arranges in a 1D cluster chain. Complex **5** exhibits a 2D layered structure characterized by 3,4,3-connected $(4.6^2)_3(4.6^3.8^2)(4^2.6^3.8)(4^2.6)$ topology. Complex **6** possesses a 3D network with **sra** topology. The magnetic properties of complexes **1** and **4** were investigated.

Introduction

Coordination polymers have recently attracted much attention because of their fascinating structures and their potential application in magnetism, luminescence, adsorption, catalysis, *etc*.[1] Research has mainly focused on homometallic systems. However, heterometallic coordination polymers, which often exhibit novel electromagnetic properties, remain relatively scarce because of the coordinative complexity of the heterometallic ions involved in the self-assembly process.[2] Up to date, there are two main synthetic approaches to obtain the heterometallic coordination polymers. One is a one-pot synthetic approach. Adopting this synthetic approach, the ligand design strategy is very important in the construction of unusual heterometallic coordination frameworks.[3–5] However, the design and synthesis of heterometallic polymers is still a challenge to chemists, especially in the case of 3d–3d heterometallic polymers, because a one-pot synthetic approach can lead to a statistical mixture of homo- and heterometallic architectures.[6] The other synthetic approach is given by the concept of 'complex ligand', *i.e.*, utilizing a metal complex as a ligand to coordinate an appropriate additional metal ion.[7–10] A good example is represented by the use of mononuclear oxamide group complexes.[9]

The macrocyclic oxamides, in which the *exo–cis* conformation of the oxygen donors is enforced, allow us to synthesize heterobimetallic systems and model magnetic systems in a more controlled fashion *via* the stepwise complexation of the macrocyclic and *exo* donors (Scheme 1a).[11] However, heterobimetallic coordination polymers based on macrocyclic oxamides are rarely obtained, because of the limitations of the coordination modes of the macrocyclic oxamide. So the construction of heterobimetallic coordination polymers containing macrocyclic oxamides requires other co-ligands with one or more bridges. Recently, our groups have succeeded in the synthesis of some oxamido-bridged macrocyclic coordination polymers with N_3^-, SCN^-, $N(CN)_2^-$, ClO_4^- and 5-sulfosalicylic acid co-ligands.[12] Although some oxamido-bridged coordination polymers have been synthesized, rational control in the construction of polymeric networks still remains a great challenge in crystal engineering. Heterometallic polymers with multi-dimension have been made rarely.[12] Therefore, in order to design and construct the diverse multi-dimension oxamido-bridged heteropolynuclear network, we have chosen the 1,3,5-benzenetricarboxylic acid as co-ligand, because it has a great ability to adopt different bonding modes and satisfy many

[a]*Tianjin Key Laboratory of Structure and Performance for Functional Molecule, College of Chemistry, Tianjin Normal University, Tianjin, 300387, P. R. China. E-mail: hxxysyq@mail.tjnu.edu.cn; Tel: (86)-22-81585464*
[b]*Department of Chemistry, Nankai University, Tianjin, 300071, P. R. China. E-mail: liaodz@nankai.edu.cn*
[c]*Tianjin University of Science & Technology, Sch Sci, Tianjin, P. R. China*
† Electronic supplementary information (ESI) available. CCDC reference numbers 800812–800817. For ESI and crystallographic data in CIF or other electronic format see DOI: 10.1039/c0dt01584a

 This journal is © The Royal Society of Chemistry 2011

Published on 19 April 2011. Downloaded by Heinrich Heine University of Duesseldorf on 24/05/2013 13:04:26.

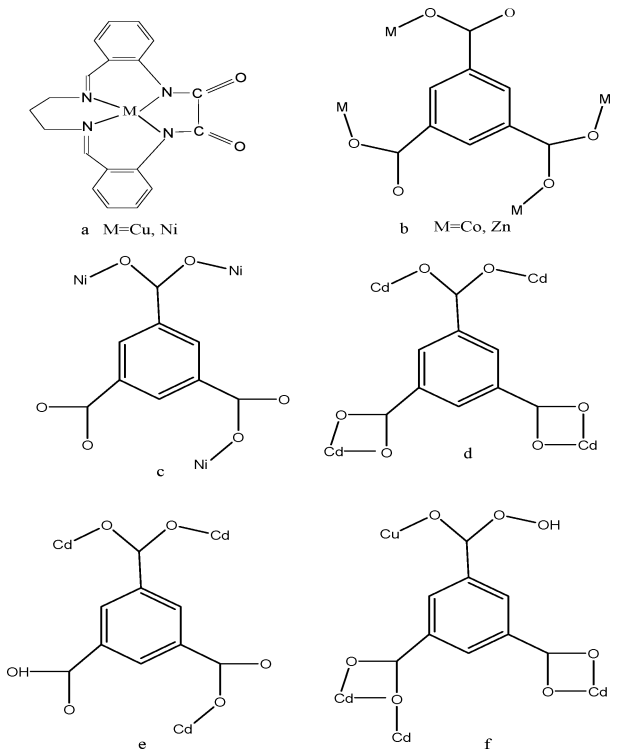

Scheme 1 The macrocyclic oxamide complex ligands and coordinated modes of the 1,3,5-benzenetricarboxylate.

metal coordination preferences.[13] Meanwhile, the employment of the metal ions Cu^{II}, Co^{II}, Zn^{II}, Ni^{II}, Cd^{II}, which have different electronic structures, sizes, hard/soft behaviours, could lead to the diversity and complexity of the resulted heterometallic assemblies and new functional properties. The results show that the marrying of the ML macrocyclic units with the tritopic BTC^{3-} and/or $HBTC^{2-}$ ligands has indeed led to interesting and novel 1, 2 and 3D extended networks. Herein, we report the syntheses, structures, topological analysis, and properties of six coordination polymers $[M'_4(BTC)_2(ML)_2(OH)_2(H_2O)_2]\cdot 2H_2O$ (M′ = Co, M = Ni, for (**1**); M′ = Zn, M = Ni, for (**2**); M′ = Zn, M = Cu, for (**3**)), $[Ni_3(BTC)_2(NiL)_2(H_2O)_6]\cdot 2CH_3OH\cdot 2H_2O$ (**4**), $[Cd_4(BTC)_2(HBTC)(NiL)_4(H_2O)]\cdot 3H_2O$ (**5**) and $[Cd(HBTC)(CuL)]\cdot H_2O$ (**6**).

Experimental

Materials and physical measurements

All the starting reagents were of A. R. grade and were used as purchased. The complex ligand ML(M = Cu, Ni) was prepared as described elsewhere.[14] Analyses of C, H and N were determined on a Perkin–Elmer 240 Elemental analyzer. IR spectrum was recorded as KBr discs on a Shimadzu IR-408 infrared spectrophotometer in the 4000–600 cm^{-1} range. XRPD spectra for the power were recorded with a Model D/MAX-2550V, Rigaku, Japan. Variable-temperature magnetic susceptibilities of single crystals were measured on an MPMS-7 SQUID magnetometer. Diamagnetic corrections were made with Pascal's constants for all the constituent atoms.[15]

X-Ray crystallography

Single crystal X-ray diffraction analyses of **1–6** were carried out on a Bruker Smart Apex II CCD diffractometer equipped with a graphite monochromated Mo–Kα radiation (λ = 0.71073 Å) by using a ϕ/ω scan technique at room temperature. Semi-empirical absorption corrections were applied using SADABS. All structures were solved by direct methods using the SHELXS program of the SHELXTL package and refined with SHELXL. The crystallographic data and selected bond lengths and angles for **1–6** are listed in Table 1–3. CCDC reference numbers: 800812–800817.

Preparation of complexes of 1–6

Caution! Perchlorate salts of metal complexes with organic ligand are potentially explosive and should be handled with care in small quantities.

Synthesis of $[M_4(BTC)_2(NiL)_2(OH)_2(H_2O)_2]\cdot 2H_2O$ (M = Co, 1; Zn, 2). A mixture of $M(ClO_4)_2\cdot 6H_2O$ (0.05 mmol, M = Co, **1**; Zn, 2), H_3BTC (0.05 mmol, 10.5 mg), NiL (0.025 mmol, 9.8 mg), H_2O (10 mL) and CH_3OH (3 mL) was stirred for 40 min at room temperature, and the pH value of the solution was adjusted to about 7–8 with triethylamine. After stirring, the mixture was transferred to an 18 ml Teflon-lined reactor, and heated at 150 °C for 72 h. Then the reaction system was cooled to room temperature during 36 h, and deep red crystals for **1** and brown red crystals for **2** were isolated (for **1**, yield = 63.5% based on Co; for **2**, yield = 53.8% based on Zn) by filtering and washing with water. Calcd for $C_{28}H_{24}Co_2N_4NiO_{11}$ **1**: C, 43.69; H, 3.12; N, 7.28%. Found: C, 43.66; H, 3.09; N, 7.31%. Calcd for $C_{28}H_{24}NiN_4O_{11}Zn_2$ **2**: C, 42.97; H, 3.07; N, 7.16%. Found: C, 42.96; H, 3.05; N, 7.14%. Main IR bands (KBr, cm^{-1}): 3428 s (br), 1629 s, 1576 s, 1486 w, 1442 m, 1368 s, 1274 w, 1219 w, 1168 w, 1090 w, 767 m, 718 m, 562 w, 459 w.

Synthesis of $[Zn_4(BTC)_2(CuL)_2(OH)_2(H_2O)_2]\cdot 2H_2O$ (3). The synthetic procedure was similar to that described for the preparation of **2** except using CuL (0.025 mmol, 9.9 mg) instead of NiL. Deep brown–green crystals of **3** were obtained (yield = 63.5% based on Zn). Calcd for $C_{28}H_{24}CuN_4O_{11}Zn_2$ **3**: C, 42.71; H, 3.05; N, 7.12%. Found: C, 42.69; H, 3.02; N, 7.08%. Main IR bands (KBr, cm^{-1}): 3432 s (br), 1613 s, 1568 s, 1482 w, 1437 m, 1364 s, 1164 m, 1105 m, 767 s, 714 s, 584 m, 454 w.

Synthesis of $[Ni_3(BTC)_2(NiL)_2(H_2O)_6]\cdot 2CH_3OH\cdot 2H_2O$ (4). A mixture of $Ni(ClO_4)_2\cdot 6H_2O$ (0.05 mmol, 18.3 mg), H_3BTC (0.03 mmol, 6.3 mg), NiL (0.03 mmol, 11.8 mg), H_2O (10 mL) and CH_3OH (3 mL) was stirred for 40 min at room temperature, and the pH value of the solution was adjusted to about 7–8 with triethylamine. After stirring, the mixture was transferred to an 18 ml Teflon-lined reactor, and heated at 150 °C for 72 h. Deep brown–red crystals of **4** were obtained (yield = 63.5% based on Ni). Calcd for $C_{29}H_{31}N_4Ni_{2.50}O_{13}$ **4**: C, 44.03; H, 3.92; N, 7.09%. Found: C, 44.06; H, 3.97; N, 7.08%. Main IR bands (KBr, cm^{-1}): 3443 s (br), 1622 s, 1563 s, 1484 m, 1436 s, 1366 s, 1279 w, 1222 w, 1107 w, 1097 w, 1014 w, 970 w, 930 w, 769 s, 718 s, 590 w, 507 w, 459 w.

Synthesis of $[Cd_4(BTC)_2(HBTC)(NiL)_4(H_2O)]\cdot 3H_2O$ (5). A mixture of $Cd(ClO_4)_2\cdot 6H_2O$ (0.05 mmol, 20.9 mg), H_3BTC

View Article Online

Published on 19 April 2011. Downloaded by Heinrich Heine University of Duesseldorf on 24/05/2013 13:04:26.

Table 1 Crystal data and structure refinement for complexes **1–3**

Complexes	**1**	**2**	**3**
Formula	$C_{28}H_{24}Co_2N_4NiO_{11}$	$C_{28}H_{24}N_4NiO_{11}Zn_2$	$C_{28}H_{24}CuN_4O_{11}Zn_2$
Fw	769.08	781.96	786.79
Crystal system	Triclinic	Triclinic	Triclinic
Space group	$P\bar{1}$	$P\bar{1}$	$P\bar{1}$
a	10.149(7)	10.1145(5)	10.1376(6)
b	12.422(9)	12.3815(6)	12.3611(8)
c	13.888(10)	13.7981(6)	13.8352(8)
α (°)	100.960(13)	100.4750(10)	100.5220 (10)
β (°)	108.179(12)	107.9830(10)	107.4860(10)
γ (°)	109.137(12)	109.2310(10)	109.1880(10)
V (Å^3)	1485.8(18)	1472.49(12)	1483.59(16)
Z	2	2	2
ρ_{caled} (g cm^{-3})	1.719	1.764	1.761
v (Mo–Kα) (mm^{-1})	0.71073	0.71073	0.71073
Crystal size (mm)	0.28 × 0.22 × 0.20	0.32 × 0.22 × 0.20	0.20 × 0.10 × 0.08
T (K)	296(2)	296(2)	296(2)
Goodness-*F*^{2}	0.980	1.074	1.039
Reflections collected/unique	7420/5175	7648/5166	7594/5196
R(int)	0.0477	0.0146	0.0115
$R1^a$ [$I > 2\sigma(I)$]	0.0721	0.0298	0.0267
$wR2^b$ [$I > 2\sigma(I)$]	0.1844	0.0722	0.0660
CCDC numbers	800816	800812	800817

^{a} $R1 = \sum\|F_o| - |F_c\|/\sum|F_o|$. ^{b} $wR2 = \{\sum[w(F_o^2 - F_c^2)^2]/\sum[w(F_o)^2]\}^{1/2}$

Table 2 Crystal data and structure refinement for complexes **4–6**

Complexes	**4**	**5**	**6**
Formula	$C_{29}H_{31}N_4Ni_{2.50}O_{13}$	$C_{103}H_{82}Cd_4N_{16}Ni_4O_{30}$	$C_{28.5}H_{22}CdCuN_4O_{8.5}$
Fw	790.35	2708.29	732.44
Crystal system	Triclinic	Monoclinic	Monoclinic
Space group	$P\bar{1}$	$P2_1$	$P2_1/n$
a	9.7772(6)	18.4200(7)	10.021(3)
b	12.0096(7)	14.3984(6)	13.739(4)
c	14.0441(9)	18.8098(8)	18.812(5)
α (°)	88.6690(10)	90	90
β (°)	82.8440(10)	97.4300(10)	91.981(4)
γ (°)	71.6580(10)	90	90
V (Å^3)	1552.87(16)	4946.8(3)	2588.6(12)
Z	2	2	4
ρ_{caled} (g cm^{-3})	1.690	1.818	1.879
v (Mo–Kα) (mm^{-1})	0.71073	0.71073	0.71073
Crystal size (mm)	0.28 × 0.22 × 0.20	0.28 × 0.22 × 0.20	0.38 × 0.32 × 0.22
T (K)	296(2)	296(2)	296(2)
Goodness-*F*^{2}	1.027	1.044	1.031
Reflections collected/unique	8054/5464	25658/13515	16858/7003
R(int)	0.0157	0.0186	0.0210
$R1^a$ [$I > 2\sigma(I)$]	0.0335	0.0310	0.0289
$wR2^b$ [$I > 2\sigma(I)$]	0.0758	0.0794	0.0623
Flack parameter		0.489(16)	
CCDC numbers	800814	800815	800813

^{a} $R1 = \sum\|F_o| - |F_c\|/\sum|F_o|$. ^{b} $wR2 = \{\sum[w(F_o^2 - F_c^2)^2]/\sum[w(F_o)^2]\}^{1/2}$

(0.04 mmol, 8.4 mg), NiL (0.05 mmol, 19.6 mg), H_2O (10 mL) and CH_3OH (3 mL) was stirred for 40 min at room temperature, and the pH value of the solution was adjusted to about 6–7 with triethylamine. After stirring, the mixture was transferred to an 18 ml Teflon-lined reactor, and heated at 150 °C for 72 h. Then the reaction system was cooled to room temperature during 36 h, and brown–red crystals of the compound **5** were isolated (yield = 73.5% based on Cd) by filtering and washing with water. Calcd for $C_{103}H_{82}Cd_4N_{16}Ni_4O_{30}$ **5**: C, 45.64; H, 3.03; N, 8.27%. Found: C, 45.66; H, 3.07; N, 8.28%. Main IR bands: 3416 s (br), 1718 m, 1629 s, 1588 s, 1565 s, 1478 m, 1433 s, 1368 s, 1319 m, 1278 m, 1162 w, 1099 w, 1074 w, 976 w, 914 w, 813 w, 767 s, 730 s.

Synthesis of [Cd(HBTC)(CuL)]·H_2O (6). A mixture of $Cd(ClO_4)_2·6H_2O$ (0.05 mmol, 20.9 mg), H_3BTC (0.05 mmol, 10.5 mg), CuL (0.05 mmol, 20.4 mg), H_2O (10 mL) and CH_3OH (3 mL) was stirred for 40 min at room temperature, and the pH value of the solution was adjusted to about 6–7 with triethylamine. After stirring, the mixture was sealed in an 18 mL Teflon-lined reactor which was kept at 150 °C for 72 h. Deep brown–green

 This journal is © The Royal Society of Chemistry 2011

View Article Online

Published on 19 April 2011. Downloaded by Heinrich Heine University of Duesseldorf on 24/05/2013 13:04:26.

Table 3 Selected bond distances (Å) and angles (°) for **1**, **4–6**[a]

Compound **1**			
Ni(1)–N(4)	1.877(7)	Ni(1)–N(1)	1.909(6)
Co(1)–O(10)	2.084(5)	Co(1)–O(9)#1	2.087(5)
Co(1)–O(9)	2.090(5)	Co(1)–O(2)	2.090(5)
Co(1)–O(5)#2	2.097(5)	Co(1)–O(1)	2.112(5)
Co(2)–O(8)#3	1.944(6)	Co(2)–O(9)	1.946(4)
Co(2)–O(3)	1.949(6)	Co(2)–O(6)#2	1.974(5)
N(4)–Ni(1)–N(2)	165.9(3)	N(2)–Ni(1)–N(1)	86.7(3)
O(2)–Co(1)–O(5)#2	82.1(2)	O(10)–Co(1)–O(5)#2	176.5(2)
O(10)–Co(1)–O(9)	91.4(2)	O(8)#3–Co(2)–O(6)#2	102.1(2)
O(9)–Co(2)–O(3)	116.4(2)	O(9)–Co(2)–O(6)#2	107.1(2)
Compound **4**			
Ni(1)–O(3)	2.0558(19)	Ni(1)–O(6)#2	2.0718(18)
Ni(1)–O(9)	2.1452(18)	Ni(2)–O(5)#2	2.009(2)
Ni(2)–O(1)	2.067(2)	Ni(2)–O(9)	2.0888(18)
Ni(3)–N(4)	1.877(3)	Ni(3)–N(1)	1.908(3)
O(3)–Ni(1)–O(3)#1	180.00(16)	O(3)–Ni(1)–O(9)#1	88.34(7)
O(1)–Ni(2)–O(11)	82.86(9)	O(2)–Ni(2)–O(9)	174.27(8)
O(5)#2–Ni(2)–O(9)	95.62(8)	N(2)–Ni(3)–N(1)	90.96(12)
N(4)–Ni(3)–N(1)	94.54(12)	N(4)–Ni(3)–N(2)	166.56(12)
Compound **5**			
Cd(1)–O(9)	2.228(4)	Cd(1)–O(13)#1	2.567(5)
Cd(2)–O(16)	2.193(5)	Cd(2)–O(21)	2.521(5)
Cd(3)–O(23)	2.198(4)	Cd(3)–O(12)	2.428(4)
Cd(4)–O(24)	2.211(4)	Cd(4)–O(26)#3	2.529(5)
Ni(1)–N(4)	1.880(8)	Ni(1)–N(3)	1.892(8)
O(9)–Cd(1)–O(1)	80.52(16)	O(9)–Cd(1)–O(2)	149.05(18)
O(16)–Cd(2)–O(4)	85.59(16)	O(16)–Cd(2)–O(3)	156.44(17)
O(18)#2–Cd(3)–O(7)	165.27(17)	O(18)#2–Cd(3)–O(11)	90.85(18)
O(25)#3–Cd(4)–O(27)	80.21(19)	O(24)–Cd(4)–O(6)	143.25(18)
N(2)–Ni(1)–N(1)	86.8(2)	N(4)–Ni(1)–N(2)	163.8(3)
Compound **6**			
Cd(1)–O(7)#1	2.2448(18)	Cd(1)–O(2)	2.2531(18)
Cd(1)–O(8)#1	2.515(2)	Cd(1)–O(3)	2.6283(19)
Cu(1)–N(1)	1.962(2)	Cu(1)–N(4)	2.021(2)
O(4)–Cd(1)–O(3)	52.63(6)	O(8)#1–Cd(1)–O(3)	162.42(6)
O(7)#1–Cd(1)–O(2)	139.61(8)	O(7)#1–Cd(1)–O(3)#2	110.69(7)
O(2)–Cd(1)–O(1)	70.27(6)	O(2)–Cd(1)–O(8)#1	94.11(7)
O(2)–Cd(1)–O(3)	81.64(7)	N(1)–Cu(1)–N(3)	172.61(9)
N(1)–Cu(1)–N(2)	82.96(8)	N(3)–Cu(1)–N(4)	95.56(10)

[a] Symmetry transformations:**1**:#1 $-x, -y, -z$; #2 $x-1, y, z$; #3 $-x+1, -y+1, -z$. **4**: #1 $-x+2, -y, -z$; #2 $x-1, y, z$. **5**: #1 $-x+1, y-1/2, -z+1$; #2 $x, y+1, z$; #3 $-x, y+1/2, -z+2$. **6**: #1 $x-1, y, z$; #2 $-x, -y+1, -z$.

crystals of **6** were obtained (yield = 60.3% based on Cd). Calcd for $C_{28}H_{22}CdCuN_4O_9$ **6**: C, 46.69; H, 3.00; N, 7.63%. Found: C, 46.70; H, 3.02; N, 7.66%. Main IR bands (KBr, cm^{-1}): 3432 s (br) 1689 m, 1613 s, 1572 s, 1485 w, 1438 m, 1362 m, 1275 w, 1162 w, 1101 w, 976 w, 914 w, 750 m, 720 m, 681 w, 592 w, 466 w.

Results and discussion

Synthetic and spectral aspects

By using 1,3,5-benzenetricarboxylic acid and macrocyclic oxamide mixed ligands as the metal linker, six new complexes have been synthesized under solvothermal conditions. The results reported here and previously reported[12g,12h] clearly show that the solvothermal synthesis is a powerful and versatile tool for preparing macrocyclic oxamide and organic acid bridged heterometallic coordination polymers. Considering that the deprotonated degree of H_3BTC may play a vital role in constructing the extended structures, a series of experiments were performed varying the pH values of the reaction system in the range of 4–9. The results show that complexes for **1–4** were obtained at relatively higher pH (7–8), whereas compounds **5** and **6** were obtained at relatively lower pH (6–7). In order to explore the effect of the other reaction parameters in preparing complexes **1–6**, a large numbers of experiments were also carried out *via* varying the reaction temperature (100 to 180 °C) and time (1 to 4 days), and the results show that single-crystal products suitable for X-ray analysis can only be readily obtained at 150 °C for 3 days.

For complexes **1–6**, the spectra exhibit strong absorption bands in the region 1629–1613 cm^{-1} and 1588–1563 cm^{-1} due to the υ(C=O) and the υ(C=N) vibrations, respectively.[16,17] The IR spectra of **1**, **2**, **3** and **4** show no bands in the region 1680–1720 cm^{-1}, indicating complete deprotonation of the carboxyl groups. While the IR spectra of the complexes **5** and **6** show one band around 1718 cm^{-1} in **5**, and around 1689 cm^{-1} in **6**, which are characteristic of the protonation of the carboxyl groups.[17] The IR spectra of **1**, **2**, **3**, **4** and **5** exhibit broad absorption bands in the range 3260–3450 cm^{-1}, indicating the existence of coordinated water.[17] To confirm the phase purity of the obtained complexes, the original samples were characterized

Published on 19 April 2011. Downloaded by Heinrich Heine University of Duesseldorf on 24/05/2013 13:04:26.

by XRPD at room temperature. The experimental spectra (Fig. S1†) of complexes **1**, **2**, **4** and **5** are almost consistent with those simulated based on the structure models derived from single-crystal X-ray diffraction data, indicating the phase purity of the products.

Structural description

The ligands involved in this research and coordination modes of 1,3,5-benzenetricarboxylate ligand are listed in Schemes 1.

$[Co_4(BTC)_2(NiL)_2(OH)_2(H_2O)_2]\cdot 2H_2O$ (1)

Compounds **1–3** are isomorphous, hence only the structure of **1** will be discussed in detail as a representative. Single-crystal X-ray analyses revealed that the complex **1** crystallizes in the triclinic space group $P\bar{1}$. The asymmetric unit of **1** consists of one copper(II) ion, two cobalt(II) ions, one macrocyclic oxamide group, one BTC^{3-}, two water molecules, and one hydroxyl (Fig. S2†). The complex **1** is a 2D layer coordination polymer composed of hexanuclear Co_4Ni_2 building unit $[Co_4(BTC)_2(NiL)_2(OH)_2(H_2O)_2]$. As shown in Fig. 1a, in the hexanuclear structure of **1**, the nickel ion is coordinated by four nitrogen atoms from the macrocyclic organic ligand, with the $[NiN_4]$ geometry exhibiting a distorted square planarity. The Co(1) ion is six-coordinated by two oxygen atoms from one oxamido ligand (Co(1)–O(1) = 2.113(5) and Co(1)–O(2) = 2.091(5) Å), one oxygen atom from a BTC^{3-} (Co(1)–O(5) = 2.097(5) Å), one oxygen atom from a water molecule (Co(1)–O(10) = 2.084(5) Å), and two oxygen atoms from two μ_3-OH groups (Co(1)–O(9) = 2.090(5) and Co(1)–O(9A) = 2.087(5) Å). However, the Co(2) ion is tetrahedrally surrounded by one μ_3-OH group (Co(2)–O(9) = 1.946(4) Å) and three oxygen atoms (Co(2)–O(3) = 1.949(6), Co(2)–O(6B) = 1.974(5) and Co(2)–O(8C) = 1.944(6) Å) belonging to three different carboxylate groups from three separated BTC^{3-} ligands. The Co(2)–O average bond length (1.953(5) Å) is somewhat shorter than those of Co(1)–O (2.093(5) Å) and this is consistent with the fact that bond lengths in a tetrahedral geometry are generally shorter than those in other geometries. Four adjacent metal ions (Co(1), Co(2), Co(1A), Co(2A)) are connected by two bridging μ_3-OH groups to construct a tetrametallic cluster $[Co_4(\mu_3\text{-}OH)_2]$, in which the non-bonding distances of Co···Co are 3.359(6) Å (Co(1)···Co(2)), 3.543(4) Å (Co(1)···Co(2A)), and 3.102(4) Å (Co(1)···Co(1A)), respectively. Nickel ions and the $[Co_4(\mu_3\text{-}OH)_2]$ cluster are interlinked through the macrocyclic oxamide ligand to form a hetero-hexanuclear Co_4Ni_2 unit. The structural Co_4Ni_2 building units are further linked with each other through the BTC^{3-} to create an infinite 2D layer with the formula $[Co_4(BTC)_2(NiL)_2(OH)_2(H_2O)_2]\cdot 2H_2O$ (Fig. 1b). In the 2D layer structure, the BTC^{3-} act as a tetradentate connector to bridge four Co(II) ions (Scheme 1b).

From the topological view of the complex **1**, the 2D layer consists of $[Co_4(\mu_3\text{-}OH)_2]$ clusters, and each Co_4 unit is connected through six carboxylate groups. Consequently, the Co_4 unit can be viewed as an irregular six-connected node. Each BTC^{3-} ligand connects three Co_4 units, so BTC^{3-} ligands are 3-connected nodes. Thus, as illustrated in Fig. 1c, polymer **1** affords a (3,6)-connected dinodal two-dimensional (2D) network with a $(4^3)_2(4^6.6^6.8^3)$ topology.

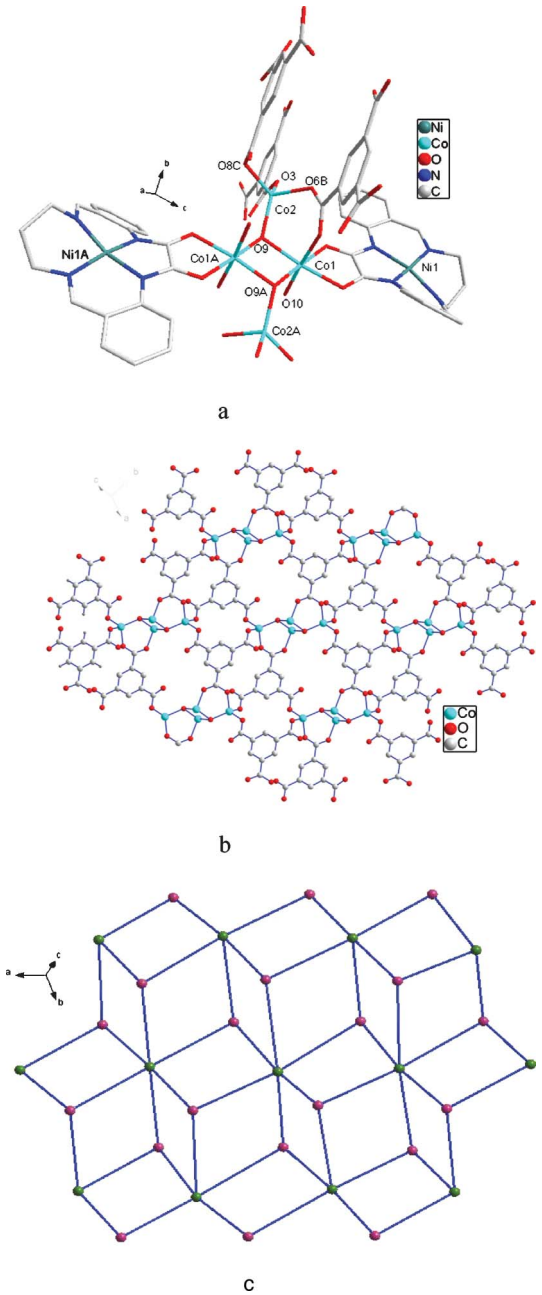

Fig. 1 (a) Portion of the crystal structure of **1** showing the coordinate environments of Co(II) and Ni(II) ions; all H atoms are omitted for clarity (symmetry code: A $-x$, $-y$, $-z$; B $x-1$, y, z; C $-x+1$, $-y+1$, $-z$). (b) View of the self-assembly 2D sheet structure constructed by $[Co_4(BTC)_2(NiL)_2(OH)_2(H_2O)_2]$; hydrogen atoms, coordinated water and NiL ligands were removed for clarity. (c) The topological representation of the 2D sheet; the green and red balls represent $[Co_4(\mu_3\text{-}OH)_2]$ and BTC^{3-} units, respectively.

$[Ni_3(BTC)_2(NiL)_2(H_2O)_6]\cdot 2CH_3OH\cdot 2H_2O$ (4)

Complex **4** crystallizes in the triclinic space group $P\bar{1}$. The asymmetric unit of **4** consists of two and half nickel(III) ions, one macrocyclic oxamide group, one BTC^{3-}, four water molecules, and one methanol molecule (see Fig. S3†). The structure of **4** is a 1D double chain coordination polymer consisting of pentanuclear Ni_5 building blocks. As shown in Fig. 2a, the Ni(1) ion is coordinated

 This journal is © The Royal Society of Chemistry 2011

Published on 19 April 2011. Downloaded by Heinrich Heine University of Duesseldorf on 24/05/2013 13:04:26.

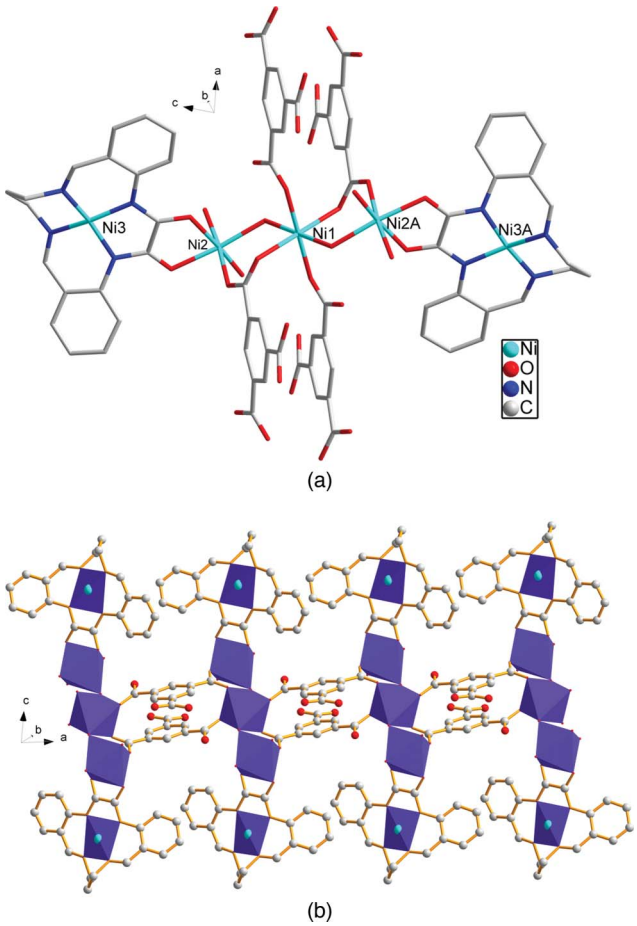

Fig. 2 (a) Portion of the crystal structure of **4** showing coordinate environments of Ni(II) ions; all H atoms are omitted for clarity (symmetry code: A –1 + *x*, *y*, *z*). (b) The polyhedral view of the self-assembly 1D chain structure constructed by $[Ni_3(BTC)_2(NiL)_2(H_2O)_6]$; the blue polyhedrons represent Ni(II) atoms.

by four carboxylate oxygen atoms from four BTC^{3-} ligands with Ni–O distances 2.0558(19)–2.0718(18) Å, and two oxygen atoms from two water molecules (Ni(1)–O(9) = 2.1452(18) Å), showing a distorted octahedral coordination environment. The Ni(2) ion also has a distorted octahedral geometry with two oxygen atoms from one oxamido ligand, three oxygen atoms from three water molecules, a carboxylate oxygen atom from a BTC^{3-}. While the Ni(3) ion is coordinated by four nitrogen atoms from the macrocyclic organic ligand, with the $[NiN_4]$ geometry exhibiting a distorted square planarity. Three adjacent metal ions (Ni(1), Ni(2), Ni(2A)) are connected by two bridging μ_2-OH_2 groups to construct a linear trimetallic cluster $[Ni_3(\mu_2\text{-}OH_2)_2]$, in which the non-bonding distances of Ni···Ni are 3.7166(4) Å (Ni(1)···Ni(2) or Ni(1)···Ni(2A)). Ni(3) (Ni(3A)) and the $[Ni_3(\mu_2\text{-}OH_2)_2]$ cluster are interlinked through the macrocyclic oxamide ligand to form a pentanuclear Ni_5 unit. Adjacent pentanuclear units are connected by two BTC^{3-} bridging ligands to form a 1D infinite chain, as shown in Fig. 2b. In the 1D chain structure, the BTC^{3-} acts as a tridentate connector to bridge three Ni(II) ions (Scheme 1c), and the relationship of the adjacent BTC^{3-} with respect to each other is *anti*. Furthermore, the 1D infinite chains are linked together with O–H···O hydrogen bonding to form a 2D framework along the *c* direction (Fig. S4†). The $d_{(H\cdots O)}$ and $d_{(O\cdots O)}$ distances between the chains are 1.75 and 2.6007 Å, respectively.

$[Cd_4(BTC)_2(HBTC)(NiL)_4(H_2O)]\cdot 3H_2O$ (5)

Complex **5** crystallizes in the monoclinic space group $P2_1$. The asymmetric unit of **5** consists of four cadmium(II) ions, four nickel(II) ions, four macrocyclic oxamide groups, two BTC^{3-}, one $HBTC^{2-}$, and four water molecules (Fig. S5†). As shown in Fig. 3a, in the octanuclear structure of **5** each Cd(II) ion is linked to a Ni(II) ion *via* the *exo–cis* oxygen donors of the macrocyclic oxamide ligand. The Ni(II) ion is coordinated by four nitrogen atoms from the macrocyclic organic ligand, with the $[NiN_4]$ geometry exhibiting a distorted square planarity. The Cd(1) ion is six-coordinated by two oxygen atoms from one oxamide ligand, and four carboxylate oxygen atoms from two different BTC^{3-} and one $HBTC^{2-}$. The coordination sphere of the Cd(1) ion is a distorted octahedral geometry, which can be seen from the bond angles O–Cd(1)–O varying from 53.18(15) to 149.05(18)°. The Cd(4) ion coordinates with two oxygen donors of the macrocyclic oxamide ligand, three carboxylate oxygen atoms from two different BTC^{3-} and one oxygen atom from a water molecule, with the $[Cd(1)O_6]$ unit exhibiting a distorted octahedral geometry. The coordination environment of Cd(2) and Cd(3) is similar to that of Cd(1). The adjacent Cd(1) and Cd(2) centers are connected by two carboxylate from one $HBTC^{2-}$ and one BTC^{3-}, adopting a μ_2-$\eta^1:\eta^1$ bridging mode to construct a bimetallic unit $[Cd_2(CO_2)_2]$, in which the non-bonding distance of Cd(1)···Cd(2) is 3.890(8) Å. While the adjacent Cd(3) and Cd(4) ions are connected by a carboxylate from one BTC^{3-}, adopting a μ_2-$\eta^1:\eta^1$ bridging mode to construct a bimetallic unit $[Cd_2(CO_2)]$, in which the non-bonding distance of Cd(3)···Cd(4) is 4.195(5) Å. The bimetallic units $[Cd_2(CO_2)_2]$ and $[Cd_2(CO_2)]$ are connected by bridging ligands BTC^{3-} and $HBTC^{2-}$ to form a 2D layer framework, as shown in Fig. 3b.

In the 2D frameworks, each $HBTC^{2-}$ ligand connects three Cd(II) ions with carboxylate groups, adopting μ_1-$\eta^0:\eta^1$ monodentate, and μ_2-$\eta^1:\eta^1$-bridging coordination modes, as shown in Scheme 1e and Fig. 3b. While each BTC^{3-} ligand connects four Cd(II) ions with carboxylate groups, adopting μ_1-$\eta^1:\eta^1$-chelating and μ_2-$\eta^1:\eta^1$-bridging coordination modes (see Scheme 1d). Topologically, the structure is composed of 3-connecting $HBTC^{2-}$ anions, 4-connecting BTC^{3-} anions, and 3-connecting Cd(II) ions. The complicated 3,4,3-connected 6-nodal 2D network is shown Fig. 3c. The Schläfli symbols are $(4.6^2)_3(4.6^3.8^2)(4^2.6^3.8)(4^2.6)$.

$[Cd(HBTC)(CuL)]\cdot H_2O$ (6)

Single-crystal X-ray analysis revealed that **6** is a complicated 3D framework consisting of crystallographically independent cadmium(II) and copper(II) ions (Fig. S6†), and crystallizes in the monoclinic space group $P2(1)/n$. As shown in Fig. 4a, the Cu(II) ion is five-coordinated by four nitrogen atoms from the macrocyclic organic ligand with Cu–N distances 1.962(2)–2.021(2) Å, and one oxygen atom from a $HBTC^{2-}$ (Cu–O = 2.5602(21) Å) to complete the distorted tetragonal pyramidal coordination geometry. The apical position is occupied by a carboxylate oxygen atom. The Cd(II) ion is seven-coordinated by two oxygen atoms from one oxamido ligand, and five carboxylate oxygen atoms from three different $HBTC^{2-}$, with the $[CdO_7]$ unit exhibiting a distorted

Published on 19 April 2011. Downloaded by Heinrich Heine University of Duesseldorf on 24/05/2013 13:04:26.

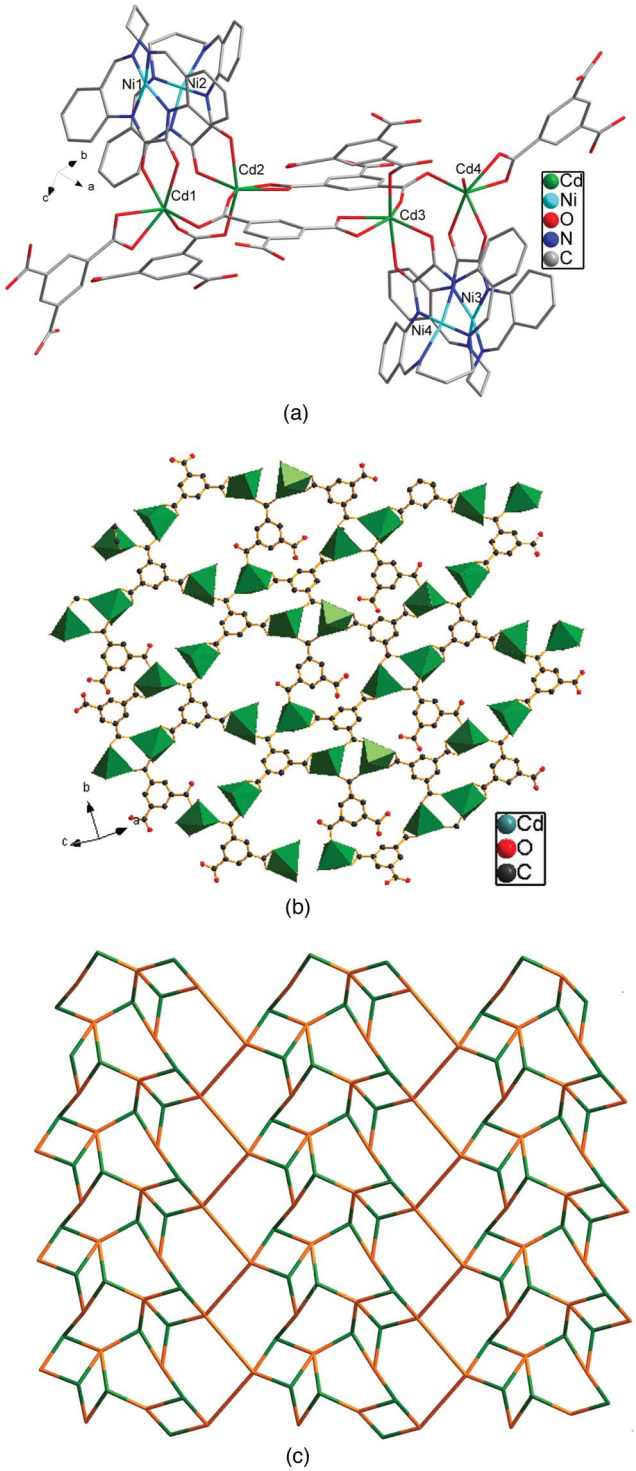

Fig. 3 (a) Portion of the crystal structure of **5** showing coordinate environments of Cd(II) and Ni(II) ions; all H atoms are omitted for clarity. (b) The polyhedral view of the self-assembly 2D sheet constructed by BTC^{3-}, $HBTC^{2-}$ and the center Cd(II) atoms; the green polyhedrons represent Cd(II) atoms; NiL ligands were removed for clarity. (c) The topological representation of the 2D sheet; the green and orange sticks represent Cd(II) atoms and 1,3,5-benzenetricarboxylate, respectively.

capped-octahedral geometry. The Cd(1)–O bond lengths range from 2.2448(18) to 2.6283(19) Å. Two adjacent cadmium(II) ions are connected by two carboxylates from two different $HBTC^{2-}$,

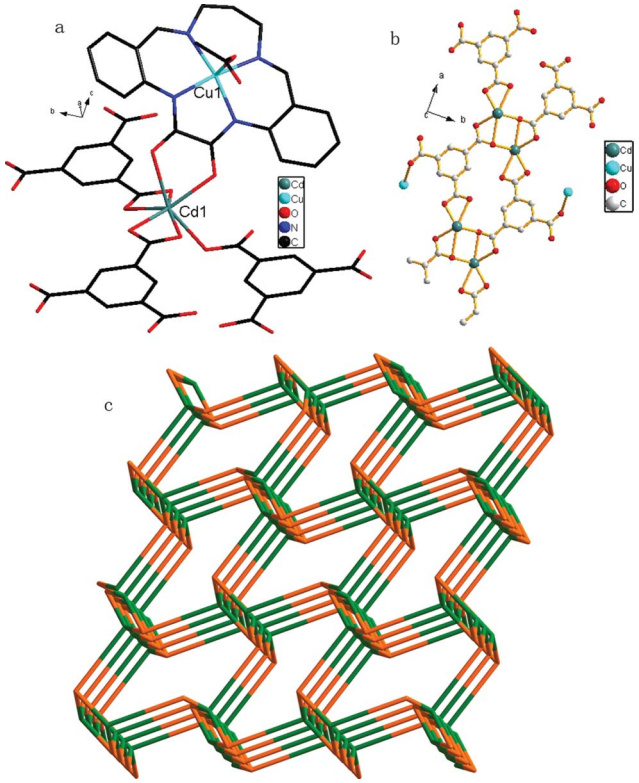

Fig. 4 (a) Portion of the crystal structure of **6** showing coordinate environments of Cd(II) and Cu(II) ions; all H atoms are omitted for clarity. (b) Portion of the crystal structure of **6** showing the coordinate environments of $HBTC^{2-}$ ligands; some C atoms of NiL ligands were removed for clarity. (c) The topological representation of the **sra** net; the green and red sticks represent Cd(II) atoms and $HBTC^{2-}$, respectively.

adopting a μ_2-$\eta^2:\eta^1$ bridging mode to construct a bimetallic cluster $[Cd_2O_2]$, in which the non-bonding distances of Cd···Cd are 3.7602(7) Å. Two Cu(II) ions and a $[Cd_2O_2]$ cluster are interlinked through the macrocyclic oxamide ligand to form a tetranuclear Cu_2Cd_2 unit. Adjacent tetranuclear Cu_2Cd_2 units are connected by bridging ligands $HBTC^{2-}$ to form 3D frameworks. In the 3D frameworks, each $HBTC^{2-}$ ligand connects four metal ions [three Cd(II) and one Cu(II)] with carboxylate groups, adopting μ_1-$\eta^0:\eta^1$ monodentate, μ_1-$\eta^1:\eta^1$-chelating, and μ_2-$\eta^2:\eta^1$-bridging coordination modes, as shown in Scheme 1f and Fig. 4b.

In the view of topology, the Cd(II) ions and $HBTC^{2-}$ ligands both are 4-connected nodes. Therefore, the whole structure can be defined as uni-nodal (4,4)-connected 3D micropore framework with Schläfli symbols ($4^2.6^3.8$), which is a typical **sra** structure (Fig. 4c). Such a structure has also been referred by to Smith as an ABW tetrahedral net in a Li–ABW zeolite and as a $SrAl_2$ net by O'Keeffe and Hyde.[18]

Magnetic Properties

The magnetization measurements for the complexes **1** and **4** have been carried out under 2 kOe. The value $\chi_M T = 9.36$ cm^3 mol^{-1} K at 300 K for powder sample **1** is larger than the spin-only value of 7.50 cm^3 mol^{-1} K expected for the uncoupled Co^{II}_4 tetranuclear system (Fig. 5). This indicates an important contribution from the orbital momentum typical for the high-spin octahedral Co^{II} with $^4T_{1g}$ ground state. On lowering the temperature, $\chi_M T$ decreases

 This journal is © The Royal Society of Chemistry 2011

Published on 19 April 2011. Downloaded by Heinrich Heine University of Duesseldorf on 24/05/2013 13:04:26.

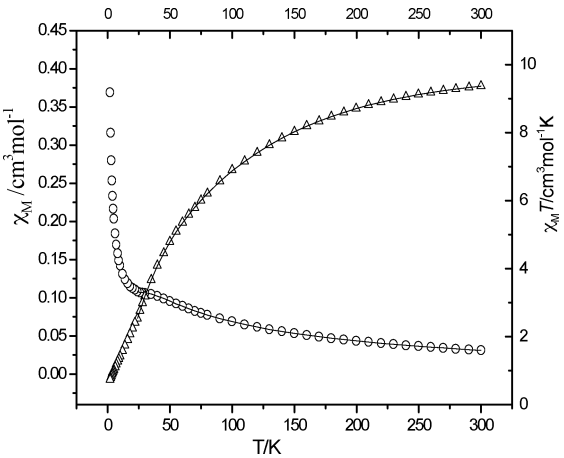

Fig. 5 χ_M (O) *versus* T and $\chi_M T$ (△) *versus* T plots for the complex **1**.

continuously and reaches 0.74 cm^3 mol^{-1} K at 2 K. The shape of the $\chi_M T$ *vs.* T curve suggests an overall antiferromagnetic behavior. On the basis of the crystal structure of **1**, Ni^{II} ion is diamagnetic in the NiL subunit, so the magnetic interactions between the cobalt and nickel ions can be neglected. Meanwhile, the magnetic interactions between the adjacent tetranuclear units $[Co_4(\mu_3\text{-}OH)_2]$ can also be neglected, because of the larger separation of Co ··· Co (about 9.62 Å). Thus, the coupling topology deduces from the crystal structure has to be considered as the Co_4 tetranuclear units shown in Scheme 2, and the contribution of the spin–orbit coupling of Co(II) ion is considered according to van Vleck's equation.[19] The magnetic analysis was carried out by using the spin Hamiltonian:

$$\hat{H} = -2J_1(\hat{S}_1\hat{S}_2 + \hat{S}_2\hat{S}_{1A} + \hat{S}_{1A}\hat{S}_{2A} + \hat{S}_{2A}\hat{S}_1) - 2J_2(\hat{S}_1\hat{S}_{1A}) + g\beta \hat{H}_Z\hat{S}_Z \quad (1)$$

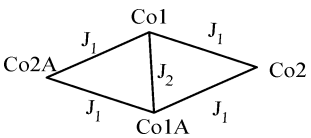

Scheme 2 The model of magnetic interaction for **1**.

The magnetic susceptibility of the tetranuclear complex can be calculated from eqn 2.

$$\chi_{tetra} = \frac{N\beta^2 g^2}{12kT} \frac{\sum_S S(S+1)(2S+1)\exp(-E(S,S_{11A})/kT)}{\sum_S (2S+1)\exp(-E(S,S_{11A})/kT)} \quad (2)$$

$$g = g_{Td} + g_{Co}(T)$$

Where, part of the orbital angular momentum of Co(II) ion is reflected in the temperature dependence of the g_{Co} factor (eqn 3).[19]

$$g_{Co} = \sqrt{\frac{3kT\chi_{Co}}{N\beta^2 S(S+1)}}$$

$$F_1 = \frac{7\lambda(3-A)^2}{5kT} + \frac{12(2+A)^2}{25A} + \left[\frac{2\lambda(11-2A)^2}{45kT} + \frac{176(A+2)^2}{27A}\right] \exp\left(\frac{-5A\lambda}{2kT}\right) + \left[\frac{\lambda(A+5)^2}{9kT} - \frac{20(A+2)^2}{27A}\right]\exp\left(\frac{-4A\lambda}{kT}\right)$$

$$F_2 = \frac{\lambda}{kT}\left[3 + 2\exp\left(\frac{-5A\lambda}{2kT}\right) + \exp\left(\frac{-4A\lambda}{kT}\right)\right] \quad (3)$$

Where J_1 and J_2 are the exchange integrals between the Co(II) and Co(II) ions. A is the ligand field parameter, and λ is the spin–orbit coupling parameter. The least-squares fit to the experimental data was found with $J_1 = -3.58$ cm^{-1}, $J_2 = -0.031$ cm^{-1}, $g_{Td} = 2.00$ (fixed), $A = 1.49$ and $\lambda = -170$ cm^- (fixed), and the agreement factor defined as $R = \Sigma(\chi_M)^{Cal} - (\chi_M)^{obsd}]^2 / \Sigma[(\chi_M)^{obsd}]^2$ is 3.52×10^{-6}. The points below 20 K can not be reproduced with this model. The magnetic behaviors below 20 K may be attributed to the intralayer and/or interlayer magnetic interactions. The weak antiferromagnetic interaction presumably originates from the high Co–O–Co angles of 122.9° or 95.98°, which differ considerably from 90°.[20]

For complex **4**, the $\chi_M T$ value is equal to 3.45 cm^3 mol^{-1} K at 300 K, which is higher than the spin-only value (3.00 cm^3 mol^{-1} K) expected for the uncoupled Ni^{II}_3 trinuclear system (Fig. 6). Upon cooling, $\chi_M T$ increases from 300 K to 17 K, and reaches a maxima of 3.64 cm^3 mol^{-1} K at 17 K. Below 17 K, $\chi_M T$ decreases quickly to 0.61 cm^3 mol^{-1} K at 2 K. This feature is characteristic of a noticeable intramolecular ferromagnetic interaction together with the effect of the zero-field splitting and/or intermolecular interaction.

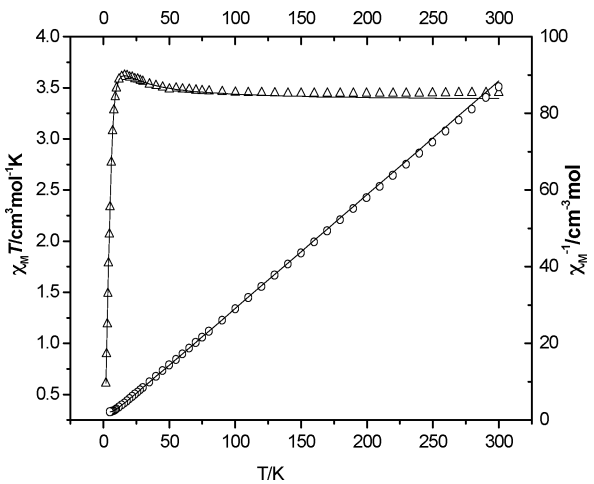

Fig. 6 χ_M^{-1}(O) *versus* T and $\chi_M T$ (△) *versus* T plots for the complex **4**.

Complex **4** is actually a 1D Ni^{II} entity formed by pentanuclear units $[Ni_3(BTC)_2(NiL)_2(H_2O)_4]$ linked by the BTC^{3-}, but Ni^{II} ion is diamagnetic in the NiL subunit. Thus, in a first approach the magnetic analysis was carried out by using the theoretical expression of the magnetic susceptibility deduced from the spin Hamiltonian

View Article Online

Published on 19 April 2011. Downloaded by Heinrich Heine University of Duesseldorf on 24/05/2013 13:04:26.

$\hat{H} = -2J(\hat{S}_1\hat{S}_2 + \hat{S}_2\hat{S}_3)$. So far as magnetic interactions between the adjacent trinuclear Ni^{II}_3 units are concerned, the molecular field approximation was used $\chi_M = \chi_{tri}/[1 - \chi_{tri}(2zj'/Ng^2\beta^2)]$. Where J is the intramolecular exchange integral between nickel(II) ions, and zj' stands for the intermolecular exchange integral of the Ni^{II}_3 units. The best-fit parameters obtained were $J = 2.69$ cm^{-1}, $g_{Ni} = 2.12$, $zj' = -0.38$ cm^{-1}, and the agreement factor defined as $R = \Sigma(\chi_M)^{Cal} - (\chi_M)^{obsd}]^2 / \Sigma[(\chi_M)^{obsd}]^2$ is 1.26×10^{-2}. The point below 6 K can not be fitted (Fig. S7†). With this hypothesis for fitting, the zj' parameter is overestimated, because the logical D parameter (zero-field splitting) was not considered.

Thus, a more realistic second approach for the magnetic analysis was carried out by using the spin Hamiltonian: $\hat{H} = -2J(\hat{S}_1\hat{S}_2 + \hat{S}_2\hat{S}_3) + D[\hat{S}_Z^2 - S(S+1)/3]\delta_{S,S} = {}_3$. So far as magnetic interactions between the adjacent trinuclear Ni^{II}_3 units are concerned, the molecular field approximation was used: $\chi_M = \chi_{tri}/[1 - \chi_{tri}(2zj'/Ng^2\beta^2)]$. Where D is a zero-field splitting parameter (assuming they are equal for each Ni^{II} ion). The least-squares fit to the experimental data was found with $J = 2.45$ cm^{-1}, $g_{Ni} = 2.12$ (fixed), $D = 2.33$ cm^{-1}, $zj' = -0.038$ cm^{-1} and the agreement factor defined as $R = \Sigma(\chi_M)^{Cal} - (\chi_M)^{obsd}]^2 / \Sigma[(\chi_M)^{obsd}]^2$ is 2.65×10^{-5}. For complex **4**, the second approach reproduces more satisfactorily the magnetic data in the whole temperature range (Fig. 6). However, this approach does not improve the fit because the inter-trinuclear magnetic coupling and D are very closely related and their independent contribution can not be easily accounted for.[21] Thus, the fitted results only indicate that, besides the intra-trinuclear coupling, the zero-field splitting and inter-trinuclear coupling are present.

The weak ferromagnetic coupling observed for complex **4** can be rationalized by the geometry parameters considerations. The interaction is predicted to be ferromagnetic for Ni–O–Ni angles lower than 93.5°, while the magnetic coupling is antiferromagnetic for greater values.[22] For complex **4**, the bond angles of Ni–O–Ni are 126.23° which usually give antiferromagnetic coupling. However, according to R. Mukherjee *et al*., when the bridging ligands are dissimilar, the ferromagnetic interaction between Ni(II) ions would result from the counter-complementary effect of the dissimilar bridges.[23] Another possible reason for the ferromagnetic interaction between the Ni(II) ions is the dihedral angles. For **4**, the two dissimilar bridges (H_2O, COO^-) destroy the planar structure of the two magnetic orbitals of the Ni(II) ions, and this distortion reduced the overlap integral that exists between the magnetic orbitals, resulting in a relatively small ferromagnetic coupling constant.

Conclusions

One homometallic and five heterometallic coordination polymers were synthesized with macrocyclic oxamide and 1,3,5-benzenetricarboxylate co-ligands under solvothermal reaction conditions. This research reveals that (i) the coexistence of macrocyclic oxamide and polycarboxylate bridged-ligands have profound effects on the construction of coordination polymers with different structures and properties; (ii) the coordination mode of the polycarboxylate groups and the coordination geometry of central metals play an important role in the structure construction. Polymers **1–6** hold the 1D, 2D or 3D framework structure, *viz*., the 1D double chains of **4**, the (3,6)-connected 2D nets of **1–3**, the (3,4,3)-connected 2D nets of **5**, and the (4,4)-connected 3D **sra**-type framework of **6**. To some extent, this work will enrich the field of coordination polymers. Further exploration of macrocyclic oxamide and polycarboxylate-bridged heterometallic materials combining multi-dimensional frameworks and interesting physical properties is currently under way in our laboratory.

Acknowledgements

This work was supported by the National Natural Science Foundation of China (No. 20771083, No. 20901059, No. 21001081, 21043004, 90922032 and No. 20771081) and National Basic Research Program of China, 978 Program, 2007CB815305.

Notes and references

1 (*a*) R. Custelcean, J. Bosano, P. V. Bonnesen, V. Kertesz and B. P. Hay, *Angew. Chem., Int. Ed.*, 2009, **48**, 4025; (*b*) X. J. Kong, Y. L. Wu, L. S. Long, L. S. Zheng and Z. P. Zheng, *J. Am. Chem. Soc.*, 2009, **131**, 6918; (*c*) Z. G. Guo, R. Cao, X. Wang, H. F. Li, W. B. Yuan, G. J. Wang, H. H. Wu and J. Li, *J. Am. Chem. Soc.*, 2009, **131**, 6894; (*d*) M. Yoshizawa, M. Tamura and M. Fujita, *Science*, 2006, **312**, 251; (*e*) S. Sato, J. Lida, K. Suzuki, M. Kawano, T. Ozeki and M. Fujita, *Science*, 2006, **313**, 1273; (*f*) S. L. James, *Chem. Soc. Rev.*, 2003, **32**, 276; (*g*) N. L. Rosi, J. Eckert, M. Eddaoudi, D. T. Vodak, J. Kim, M. O'Keeffe and O. M. Yaghi, *Science*, 2003, **300**, 1127; (*h*) O. M. Yaghi, M. O'Keeffe, N. W. Ockwig, H. K. Chae, M. Eddadoudi and J. Kim, *Nature*, 2003, **423**, 705; (*i*) S. K. Nune, P. K. Thallapally, A. Dohnalkova, C. Wang, J. Liu and G. J. Exarhos, *Chem. Commun.*, 2010, **46**, 4878; (*j*) C. A. Fernandez, P. K. Thallapally, R. K. Motkuri, S. K. Nune, J. C. Sumrak, J. Tian and J. Liu, *Cryst. Growth Des.*, 2010, **1**, 1037; (*k*) P. K. Thallapally, J. Tian, M. R. Kishan, C. A. Fernandez, S. J. Dalgarno, P. B. McGrail, J. E. Warren and J. L. Atwood, *J. Am. Chem. Soc.*, 2008, **130**, 16842.

2 (*a*) M. Westerhausen, *Dalton Trans.*, 2006, 4755; (*b*) B. Zhang, Z. H. Ni, A. L. Cui and H. Z. Kou, *New J. Chem.*, 2006, **30**, 1327; (*c*) J. R. Stork, V. S. Thoi and S. M. Cohen, *Inorg. Chem.*, 2007, **46**, 11213; (*d*) Y. Zhang, B. Chen, F. R. Fronczek and A. W. Maverick, *Inorg. Chem.*, 2008, **47**, 4433; (*e*) B. Chen, F. R. Fronczek and A. W. Maverick, *Inorg. Chem.*, 2004, **43**, 8209; (*f*) B. Chen, F. R. Fronczek and A. W. Maverick, *Chem. Commun.*, 2003, 2166.

3 (*a*) Y. C. Liang, R. Cao, W. P. Su, M. C. Hong and W. J. Zhang, *Angew. Chem., Int. Ed.*, 2000, **39**, 3304; (*b*) M. B. Zhang, J. Zhang, S. T. Zheng and G. Y. Yang, *Angew. Chem., Int. Ed.*, 2005, **44**, 1385; (*c*) Q. Yue, J. Yang, G. H. Li, G. D. Li, W. Xu, J. S. Chen and S. N. Wang, *Inorg. Chem.*, 2005, **44**, 5241; (*d*) J. W. Cheng, S. T. Zheng and G. Y. Yang, *Inorg. Chem.*, 2007, **46**, 10261; (*e*) T. K. Prasad and M. V. Rajasekharan, *Cryst. Growth Des.*, 2008, **8**, 1346.

4 (*a*) X. J. Kong, Y. P. Ren, W. X. Chen, L. S. Long, Z. P. Zheng, R. B. Huang and L. S. Zheng, *Angew. Chem., Int. Ed.*, 2008, **47**, 2398; (*b*) X. J. Kong, Y. P. Ren, L. S. Long, Z. P. Zheng, R. B. Huang and L. S. Zheng, *J. Am. Chem. Soc.*, 2007, **129**, 7016; (*c*) Q. D. Liu, S. Gao, J. R. Li, Q. Z. Zhou, K. B. Yu, B. Q. Ma, S. W. Zhang, X. X. Zhang and T. Z. Jin, *Inorg. Chem.*, 2000, **39**, 2488; (*d*) W. Shi, X. Y. Chen, Y. N. Zhao, B. Zhao, P. Cheng, A. Yu, H. B. Song, H. G. Wang, D. Z. Liao, S. P. Yan and Z. H. Jiang, *Chem.–Eur. J.*, 2005, **11**, 5031.

5 (*a*) C. E. Plenik, S. M. Liu and S. G. Shore, *Acc. Chem. Res.*, 2003, **36**, 499; (*b*) H. Z. Kou, B. C. Zhou, S. Gao and R. Z. Wang, *Angew. Chem., Int. Ed.*, 2003, **42**, 3288; (*c*) F. Prins, E. Pasca, L. J. D. Jongh, H. Kooijman, A. L. Spek and S. Tanase, *Angew. Chem., Int. Ed.*, 2007, **46**, 6081; (*d*) A. Figuerola, C. Diaz, J. Ribas, V. Tangoulis, J. Granell, F. Lloret, J. Mahía and M. Maestro, *Inorg. Chem.*, 2003, **42**, 641; (*e*) M. Estrader, J. Ribas, V. Tangoulis, X. Solans, M. Font-Bardía, M. Maestro and C. Diaz, *Inorg. Chem.*, 2006, **45**, 8239.

6 (*a*) B. Zhao, H. L. Gao, X. Y. Chen, P. Cheng, W. Shi, D. Z. Liao, S. P. Yan and Z. H. Jiang, *Chem.–Eur. J.*, 2006, **12**, 149; (*b*) O. Margeat, P. G. Lacroix, J. P. Costes, B. Donnadieu, C. Lepetit and K. N. Akatani, *Inorg. Chem.*, 2004, **43**, 4743.

7 O. Kahn, *Acc. Chem. Res.*, 2000, **33**, 647.

 This journal is © The Royal Society of Chemistry 2011

View Article Online

Published on 19 April 2011. Downloaded by Heinrich Heine University of Duesseldorf on 24/05/2013 13:04:26.

8 B. Q. Ma, S. Gao, G. Su and G. X. Xu, *Angew. Chem., Int. Ed.*, 2001, **40**, 434.
9 R. E. P. Winpenny, *Chem. Soc. Rev.*, 1998, **27**, 447.
10 D. Pogozhev, S. A. Baudron and M. W. Hosseini, *Inorg. Chem.*, 2010, **49**, 331.
11 L. Cronin, A. R. Mount, S. Parsons and N. Robertson, *J. Chem. Soc., Dalton Trans.*, 1999, 1925.
12 (*a*) S. B. Wang, G. M. Yang, D. Z. Liao and L. C. Li, *Inorg. Chem.*, 2004, **43**, 852; (*b*) X. Z. Li, L. N. Zhu, C. Q. Li and D. Z. Liao, *Inorg. Chem. Commun.*, 2006, **9**, 1297; (*c*) S. B. Wang, G. M. Yang, R. F. Li, L. C. Li and D. Z. Liao, *Inorg. Chem. Commun.*, 2004, **7**, 1082; (*d*) L. N. Zhu, N. Xu, W. Zhang, D. Z. Liao, K. Yoshimura, K. Mibu, Z. H. Jiang, S. P. Yan and P. Cheng, *Inorg. Chem.*, 2007, **46**, 1297; (*e*) S. B. Wang, G. M. Yang, R. F. Li, Y. F. Wang and D. Z. Liao, *Eur. J. Inorg. Chem.*, 2004, 4907; (*f*) Y. Q. Sun, D. Z. Gao, W. Dong, D. Z. Liao and C. X. Zhang, *Eur. J. Inorg. Chem.*, 2009, 2825; (*g*) Y. Q. Sun, L. L. Fan, D. Z. Gao, Q. L. Wang, M. Du, D. Z. Liao and C. X. Zhang, *Dalton Trans.*, 2010, **39**, 9654; (*h*) Y. Q. Sun, L. L. Fan, D. Z. Gao and G. Y. Zhang, *Z. Anorg. Allg. Chem.*, 2010, **636**, 846.
13 (*a*) Z. Su, Z. S. Bai, J. Fan, J. Xu and W. Y. Sun, *Cryst. Growth Des.*, 2009, **9**, 5190; (*b*) Y. Qi, F. Luo, Y. X. Che and J. M. Zheng, *Cryst. Growth Des.*, 2008, **8**, 606; (*c*) G. B. Che, C. B. Liu, B. Liu, Q. W. Wang and Z. L. Xu, *CrystEngComm*, 2008, **10**, 184; (*d*) F. A. A. Paz and J. Klinowski, *Inorg. Chem.*, 2004, **43**, 3948; (*e*) H. A. Habib, J. Sanchiz and C. Janiak, *Dalton Trans.*, 2008, 1734; (*f*) L. Zhang, Z. J. Li, Q. P. Lin, Y. Y. Qin, J. Zhang, P. X. Yin, J. K. Cheng and Y. G. Yao, *Inorg. Chem.*, 2009, **48**, 6517; (*g*) L. Xu, S. H. Yan, E. Y. Choi, J. Y. Lee and Y. U. Kwon, *Chem. Commun.*, 2009, 3431; (*h*) Q. R. Fang, G. S. Zhu, M. Xue, J. Y. Sun, F. X. Sun and S. L. Qiu, *Inorg. Chem.*, 2006, **45**, 3582.
14 D. S. C. Black and H. Corrie, *Inorg. Nucl. Chem. Lett.*, 1976, **12**, 65.
15 P. W. Selwood, *Magnetochemistry*, Interscience: New York, 1956; p 78.
16 F. Lloret, Y. Journaux and M. Julve, *Inorg. Chem.*, 1990, **29**, 3967.
17 K. Nakamoto, *Infrared and Raman Spectra of Inorganic and Coordination Compounds*, 5th ed.; John Wiley: New York, 1997; Part B.
18 (*a*) K. E. Holmes, P. F. Kelly and M. R. Elsegood, *Dalton Trans.*, 2004, 3488; (*b*) P. S. Wang, C. N. Moorefield, M. Panzer and G. R. Newkome, *Chem. Commun.*, 2005, 465; (*c*) L. Carlucci, G. Ciani, P. Macchi, D. M. Proserpio and S. Rizzato, *Chem.–Eur. J.*, 1999, **5**, 237; (*d*) M. O'Keeffe, M. Eddaoudi, H. L. Li, T. Reineke and O. M. Yaghi, *J. Solid State Chem.*, 2000, **152**, 3; (*e*) N. L. Rosi, M. Eddaoudi, J. Kim, M. O'Keeffe and O. M. Yaghi, *Angew. Chem., Int. Ed.*, 2002, **41**, 284.
19 F. Lioret, M. Julve, J. Cano, R. Ruiz-García and E. Pardo, *Inorg. Chim. Acta*, 2008, **361**, 3432.
20 (*a*) K. I. Okamoto, T. Konno and J. Hidaka, *J. Chem. Soc., Dalton Trans.*, 1994, 533; (*b*) P. Jaitner, J. Veciana, C. Sporer, H. Kopacka, K. Wurst and D. Ruiz-Molina, *Organometallics*, 2001, **20**, 568; (*c*) D. Q. Yuan, Y. Q. Xu, M. C. Hong, W. H. Bi, Y. F. Zhou and X. Li, *Eur. J. Inorg. Chem.*, 2005, 1182.
21 R. Boca, *Coord. Chem. Rev.*, 2004, **248**, 757.
22 (*a*) A. P. Ginsberg, R. L. Martin and R. C. Sherwood, *Inorg. Chem.*, 1968, **7**, 932; (*b*) X. H. Bu, M. Du, L. Zhang, D. Z. Liao, J. K. Tang, R. H. Zhang and M. Shionoya, *J. Chem. Soc., Dalton Trans.*, 2001, 593.
23 A. K. Sharma, F. Lloret and R. Mukherjee, *Inorg. Chem.*, 2007, **46**, 5128.